ORIGINAL ARTICLE

Crossed cerebellar diaschisis-related supratentorial hemodynamic and metabolic status measured by PET/MR in assessing postoperative prognosis in chronic ischemic cerebrovascular disease patients with bypass surgery

Bixiao Cui[1,2] · Yi Shan[1,2] · Tianhao Zhang[3,4] · Yan Ma[5] · Bin Yang[5] · Hongwei Yang[1,2] · Liqun Jiao[5] · Baoci Shan[3,4,6] · Jie Lu[1,2]

Abstract

Objective Cerebral ischemic status is an indicator of bypass surgery. Both hemodynamics and glucose metabolism are significant factors for evaluating cerebral ischemic status. The occurrence of crossed cerebellar diaschisis (CCD) is influenced by the degree of supra-tentorial perfusion and glucose metabolism reduction. This study aimed to investigate the relationship between the CCD-related supra-tentorial blood flow and metabolic status before bypass surgery in patients with chronic and symptomatic ischemic cerebrovascular disease and the prognosis of surgery.

Methods Twenty-four participants with chronic ischemic cerebrovascular disease who underwent hybrid positron emission tomography (PET)/magnetic resonance (MR) before bypass surgery were included. Arterial spin labeling (ASL)-MR and FDG-PET were used to measure blood flow and metabolism, respectively. The PET images were able to distinguish CCD. The supratentorial asymmetry index (AI) and volume in the decreased blood flow region, decreased metabolism region and co-decreased region on the affected side, except for the infarct area, were respectively obtained before bypass surgery. The neurological status was determined using the National Institutes of Health Stroke Scale (NIHSS) and modified Rankin Scale (mRS) scores. Differences between CCD-positive (CCD+) and CCD-negative (CCD−) groups were investigated.

Results Fourteen (58%) of the 24 patients were diagnosed as CCD+. Before surgery, the NIHSS and mRS scores of the CCD+ were significantly higher than those of the CCD− (1.0(1.0) vs. 0.0(1.0), $P=0.013$; 1.0(1.5) vs. 0.0(1.5), $P=0.048$). After the surgery, the NIHSS and mRS scores of the CCD+ showed a significant decrease (0.0(1.0) to 0.0(0.0), $P=0.011$; 0.0(0.5) to 0.0(0.0), $P=0.008$). Significant differences were observed in the supra-tentorial decreased metabolism region (all $Ps \leq 0.05$) between the CCD+ and CCD− groups, but no differences were observed in the preprocedural decreased supratentorial blood flow region ($P>0.05$). The preprocedural NIHSS score was strongly correlated with the metabolism AI value in the decreased metabolism region ($r=0.621$, $P=0.001$) and the co-decreased region ($r=0.571$, $P=0.004$).

Conclusions Supratentorial blood flow and metabolism are important indicators of CCD. This study showed that CCD+ patients benefited more from bypass surgery than CCD− patients. Staging based on CCD-related supra-tentorial blood flow and metabolic status by hybrid PET/MR may help to personalize treatment.

Keywords Positron emission tomography/Magnetic resonance · Glucose metabolism · Cerebral blood flow · Surgery · Crossed cerebellar diaschisis

Introduction

Data from a nationwide community-based study indicated that ischemic stroke accounts for approximately 70% of all incident stroke cases [1]. For patients with a clinical presentation of ischemic attacks and ineffective medical therapy, superficial temporal artery-middle cerebral artery

Bixiao Cui and Yi Shan contributed equally to this work.

✉ Jie Lu
imaginglu@hotmail.com

Extended author information available on the last page of the article

(STA-MCA) bypass surgery has demonstrated significant therapeutic efficacy in numerous studies [2, 3]. Several imaging studies have reported that the most crucial goal of surgical revascularization was the reduction of stroke occurrence and improvements in neurological outcomes [3, 4]. Cerebral ischemic status is an indicator of surgery. Hemodynamics and glucose metabolism are significant factors for evaluating cerebral ischemic status [5–8]. The Carotid Occlusion Surgery Study (COSS) in 2011 failed to show a clear benefit of bypass surgery in patients compared to conservative drug therapy [9]. Our previous study demonstrated that hybrid PET/MR can simultaneously measure changes in cerebral hemodynamic and metabolic patterns before and after STA-MCA bypass surgery [10]. However, we did not compare differences in the supra-tentorial hemodynamic and metabolic status before STA-MCA bypass surgery.

Crossed cerebellar diaschisis (CCD) has predominantly been studied through PET images. The incidence of CCD after supra-tentorial stroke may be 45% [11]. Baron et al. [12] first observed this phenomenon. Wang et al. [13] reported that CCD occurred due to a decrease in blood flow or metabolic activity of the related supra-tentorial region. Nocun et al. [14] showed that the degree of cerebral hypoperfusion was a determinant of CCD and correlated with the degree of cerebellar hypoperfusion in the chronic stage of stroke. Uchino et al. [15] reported that CCD may be an indicator of severe postoperative hyperperfusion in patients with chronic ischemic cerebrovascular disease. Patients with symptomatic ischemic cerebrovascular disease have a 2-year risk of subsequent ipsilateral ischemic stroke of 10–15%, but this risk increases to 25% for those with severe hemodynamic impairment [16]. The supra-tentorial hemodynamic and metabolic status plays an important role in personalizing treatment and selecting patients who will benefit the most from revascularization therapy. However, few studies describing the relationship between CCD-related supratentorial blood flow and metabolic status and bypass surgery outcomes are available.

The most important goal of surgical revascularization is to protect non-infarcted areas in which cerebral blood flow (CBF) or metabolism has decreased, as assessed by imaging. Magnetic resonance imaging (MRI) is an important diagnostic method for chronic ischemic cerebrovascular disease. Structural imaging first excludes infarcted areas. Arterial spin labeling (ASL) sequences can be used to evaluate potentially reversible tissue ischemia. ^{18}F-FDG is widely used in the measurement of brain glucose metabolism. However, various physiological processes at different time points may change between imaging sessions. Hybrid positron emission tomography (PET)/magnetic resonance (MR) is an optimal approach to simultaneously acquiring the temporal and spatial matching of datasets that display different information about a disease process. Thus, this study aimed to investigate the relationship between the CCD-related supratentorial blood flow and metabolic status before bypass surgery and the prognosis of surgery.

Materials and methods

Patients

The study was approved by the Ethics Committee of our hospital. All subjects in the study provided written informed consent for the study protocols. From October 2017 to October 2019, 24 patients were enrolled. Twenty-one of these patients were male, and 3 patients were female. The mean $\pm$ SD patient age was 49.44 ± 9.03 years (range, 32–63 years), and all subjects met the following criteria: (1) clinical diagnosis of the unilateral internal carotid artery (ICA) or MCA steno-occlusive disease that was considered severe (>70%) based on digital subtraction angiography (DSA) [5, 17]; (2) no supra-tentorial infarction (abnormal signal on T2-FLAIR images) localized in the contralateral hemisphere; (3) no structural abnormality in the cerebellum or brain stem on MR imaging (MRI); (4) a history of transient ischemic attacks or complete stroke involving the relevant ICA or MCA territory and ineffective treatment with medication; and (5) PET/MR scans less than 1 month before surgery and successful postoperative vascular connection as determined by DSA. Clinical long-term follow-up was performed for all patients with a postoperative follow-up time of at least 1 year, with an average of 21.44 months [18]. The exclusion criteria included any contraindication for MRI and artifacts on MRI.

PET/MR acquisition

Patients were evaluated before bypass surgery using a hybrid PET/MR system (Signa, GE Healthcare) with a 19-channel head and neck union coil. The glucose level of each patient was lower than 8 mmol/L. A dose of 3.7 MBq/kg ^{18}F-FDG was administered intravenously after fasting for at least 6 h before PET imaging. Fifty minutes after injection, the patients were placed into the PET/MR scanner in a supine position and instructed to remain calm with their eyes closed. ^{18}F-FDG PET images were acquired for 10 min. Attenuation correction was performed based on MR images, and the default attenuation correction sequence (Dixon MR sequences) was automatically prescribed and acquired as follows[19]: LAVA-Flex (GE Healthcare) axial acquisition, repetition time (TR) = 4 ms, echo time (TE) = 1.7 ms, slice thickness = 5.2 mm with a 2.6 mm overlap, 120 slices, pixel size = 1.95 × 2.93 mm, and acquisition time = 18 s. PET data were reconstructed into a 192 × 192 matrix, 35 cm field of view (FOV), and 2.78 mm slice thickness (voxel

size $1.82 \times 1.82 \times 2.78$ mm^3) using a time-of-flight, point spread function, ordered subset expectation maximization (TOF-PSF-OSEM) algorithm with 8 iterations, 32 subsets, and a 3 mm Gaussian filter [10].

Simultaneous PET and MRI imaging data were acquired. The sequences obtained were conventional T2WI, T1WI, T2-fluid attenuated inversion recovery (FLAIR), and 3D ASL. The following parameters were used: T2-FLAIR with 32 slices, TR = 11,000 ms, TE = 144 ms, FOV = 240×240 mm, voxel size $0.47 \times 0.47 \times 4.00$ mm^3 and scan time = 176 s and 3D ASL with 36 slices, post labeling delay (PLD) = 2550 ms, TR = 5335 ms, TE = 10.7 ms, FOV = 240×240 mm, voxel size $1.88 \times 1.88 \times 4.00$ mm^3, and scan time = 310 s.

Assessment of neurological and functional status

The National Institutes of Health Stroke Scale (NIHSS) score and the modified Rankin Scale (mRS) score were used to evaluate the neurological and functional status before the PET/MR examination as a baseline and at least at the 1-year follow-up [20, 21].

Data processing and analysis

First, two experienced doctors from the Department of Radiology and Nuclear Medicine blinded to the ASL-CBF findings visually determined CCD based on ^{18}F-FDG PET images following published criteria [22].

Second, two radiologists blinded to patient information measured the infarction area using T2-FLAIR images. For cases of disagreement, a consensus was reached in a separate session. All images were preprocessed using SPM8 (Wellcome Department of Clinical Neurology, London, UK) [10]. ^{18}F-FDG-PET and ASL images were first spatially normalized to the MNI (Montreal Neurological Institute) space with a $3 \times 3 \times 3$ mm^3 resolution using affine transformation and subsequent nonlinear warping. The ^{18}F-FDG-PET images were transformed into maps representing the radioactivity (kBq/ml), which was defined as the tissue concentration of radioactivity in each voxel normalized to the mean activity concentration. The CBF map was computed using the formula in reference [23]. All images were smoothed using an isotropic Gaussian kernel at full width at half maximum (FWHM) of 8 mm in all directions.

Parameters, including voxel-wise asymmetry index (AI) values for CBF and metabolism, were calculated after the exclusion of the infarct area from the entire supratentorial-affected side. The AI used to detect left–right asymmetry in the ^{18}F-FDG PET and ASL-CBF data is based on the following equation:

$$AI = (unaffected - affected)/unaffected \times 100\%$$

where unaffected stands for the CBF or radioactivity on the unaffected side, and affected stands for the CBF or radioactivity on the affected side. Abnormal asymmetry levels were defined as those greater than 10% [10, 22, 24].

We also defined the volume for which the voxel-wise AI value was greater than 10% as the abnormal volume, including the supratentorial decreased blood flow region, the supratentorial decreased metabolism region and the co-decreased region where both the CBF and metabolism decreased (Supplemental Fig. S1).

Statistical analysis

The reliability of visual evaluation of CCD by the two doctors was determined using the intraclass correlation coefficient (ICC). ICC value of <0.20 indicated poor agreement, ICC value of 0.21–0.40 indicated fair agreement, ICC value of 0.41–0.60 indicated moderate agreement, ICC value of 0.61–0.80 indicated good agreement, and ICC value of >0.81 indicated excellent agreement.

We performed statistical analyses using SPSS Statistics 21. The normality of the distribution was evaluated using the Shapiro–Wilk test. Normally distributed continuous variables from the CCD-positive (CCD+) and CCD-negative (CCD−) groups were compared using a two-tailed, independent-samples Student's t-test. Variables with a non-normal distribution were analyzed using the Mann–Whitney U-test. All normally distributed continuous variables are reported as medians (interquartile ranges). To identify a relationship between the parameters and neurological score using the NIHSS and mRS, we used Spearman rank-order correlation analysis. All tests were considered significant at the $P < 0.05$ level.

Results

Patient demographics and clinical characteristics

For CCD evaluation, excellent reliabilities were observed between the visual evaluation of CCD by the two doctors (ICC = 0.92; 95% confidence interval [CI] 0.82 to 0.96; $P < 0.001$). Fourteen (58%) of the 24 datasets were classified as CCD+. The CCD+ and CCD− groups did not differ significantly in age or sex. Exemplary imaging illustrations of 1 CCD+ and 1 CCD− participant are shown in Fig. 1. Detailed characteristics of the CCD+ and CCD− patients are shown in Table 1. No differences in the blood glucose or injection activity were observed between these 2 groups.
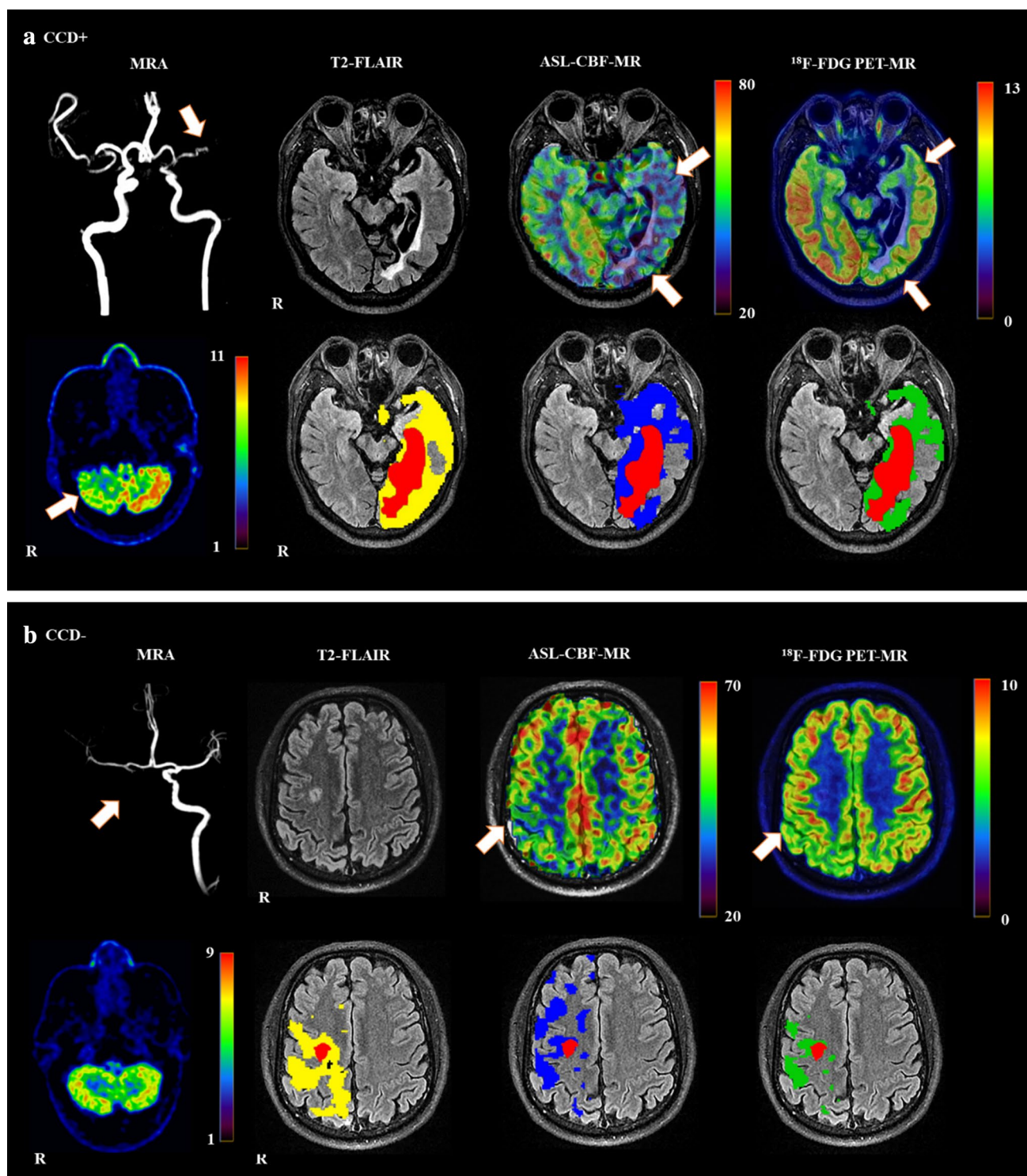
Fig. 1 Example of a CCD-positive **a** and a CCD-negative **b** participant. **a** A 44-year-old man with ischemia in the left hemisphere due to left middle cerebral artery occlusion (white arrow). On arterial spin labeling (ASL)—cerebral blood flow (CBF) imaging and ^{18}F-FDG positron emission tomography (PET), supratentorial hemodynamic and metabolic impairment may be seen in the left hemisphere (white arrows). Crossed cerebellar diaschisis (CCD) on ^{18}F-FDG PET images shown of the cerebellum (white arrow). **b** A 62-year-old man with ischemia in the right paracentral hemisphere due to right internal carotid artery occlusion (white arrow). On ASL-CBF imaging and ^{18}F-FDG PET, supratentorial metabolic and hemodynamic impairment is shown in the right hemisphere (white arrows), No CCD was observed on the cerebellar ^{18}F-FDG PET image. Red—infarct zone in the supratentorial hemisphere. Yellow—decreased blood flow regions. Blue—decreased metabolism regions. Green—co-decreased regions

Table 1 Clinical characteristics of the CCD+ and CCD− groups

	CCD+	CCD−	P value
Age	46(12)	54(14)	0.300
Male (%)	13(93)	8(80)	0.550
Preprocedural, median (IQR)			
Blood glucose (mmol/L), median (IQR)	6.00(0.85)	6.00(0.85)	1.000
Injection activity (MBq)	302.11(53.00)	295.08 (87.67)	0.403
Size of infarction, median (IQR)	962.50(1820.00)	44.00(112.75)	<0.001
Baseline			
NIHSS score, median (IQR)	1.0(1.0)	0.0(1.0)	0.013
mRS score, median (IQR)	1.0(1.5)	0.0(1.5)	0.048
Follow-up			
NIHSS score, median (IQR)	0.0(1.0)	0.0(0.0)	0.172
mRS score, median (IQR)	0.0(0.5)	0.0(0.0)	0.625

CCD crossed cerebellar diaschisis; *CBF* cerebral blood flow; *AI* asymmetry index; *IQR* interquartile range

Comparison of NIHSS and mRS between CCD-positive and CCD-negative groups

While all patients presented a favorable prognosis, the CCD+ group showed a larger change in the NIHSS and mRS scores. Before surgery, the CCD+ patients had higher preprocedural NIHSS and mRS scores than the CCD− patients (1.0(1.0) vs. 0.0(1.0), $P=0.013$; 1.0(1.5) vs. 0.0(1.5), $P=0.048$). The follow-up NIHSS and mRS scores at least 1 year after surgery were similar between

the 2 groups (0.0(1.0) vs. 0.0(0.0), $P=0.172$; 0.0(0.5) vs. 0.0(0.0), $P=0.625$). The NIHSS and mRS scores decreased significantly after surgery in the CCD+ group (0.0(1.0) to 0.0(0.0), $P=0.011$; 0.0(0.5) to 0.0(0.0), $P=0.008$, Fig. 2a, b), but no significant changes in the NIHSS and mRS scores were found in the CCD− patients (0.0(1.0) to 0.0(0.0), $P=0.157$; 0.0(1.5) to 0.0(0.0), $P=0.157$, Fig. 2c, d).

Fig. 2 Comparison of baseline and follow-up neurological scores between the two groups. Both NIHSS and mRS scores decreased after surgery in the CCD-positive (CCD+) group ($P=0.011$, $P=0.008$, Fig. 2a, b). No significant change was found in the CCD-negative (CCD−) group ($P=0.157$, $P=0.157$, Fig. 2c, d). The dots and bars stand for mean with range. **$P<0.01$, *$P<0.05$
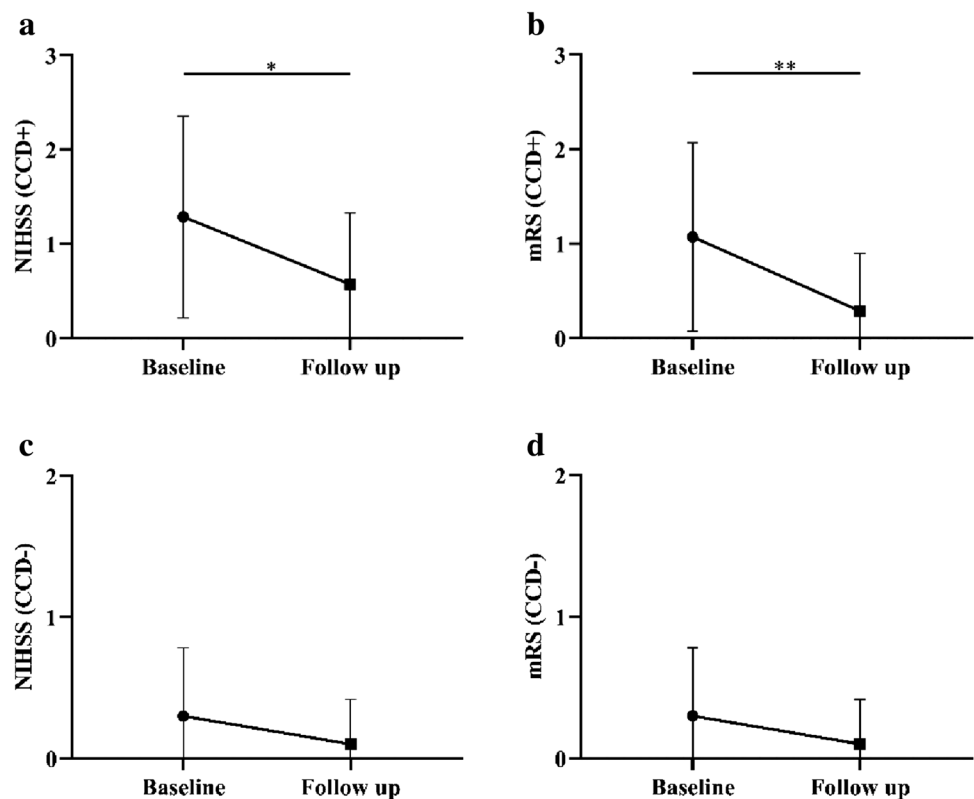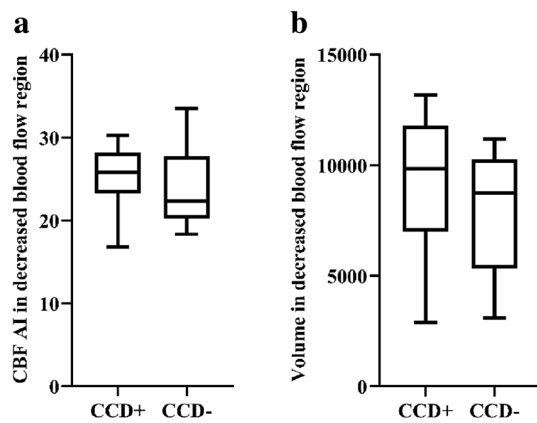
Fig. 3 Comparison of parameters in the decreased blood flow region between the two groups. No difference in either CBF AI **a** or volume **b** was observed between the CCD-positive group and the CCD-negative group

Comparison of CBF and metabolism between CCD-positive and CCD-negative groups

In the supratentorial decreased blood flow region, no statistically significant differences between the 2 groups were found in the preprocedural supratentorial CBF AI value or the volume ($P > 0.05$) (Fig. 3). In the supratentorial metabolism region, the CCD + patients showed significantly higher preprocedural supratentorial metabolism AI values and larger decreased preprocedural volume compared to the CCD− patients (CCD + vs. CCD−: 21.67 vs. 16.78, $P = 0.001$ and 9594.50 vs. 4353.00, $P < 0.001$) (Fig. 4). In the co-decreased regions which were defined as regions with decreased CBF and SUVR values, the metabolism AI and volume were also significantly higher in the CCD +
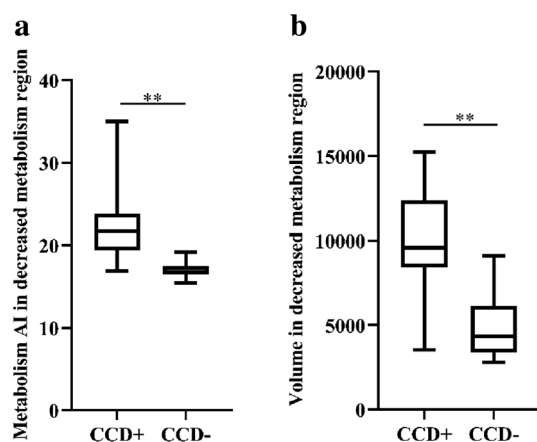

Fig. 4 Comparison of regions with decreased metabolism between the two groups. CCD-positive patients showed significantly higher metabolism AI **a** and larger volume **b** than CCD-negative patients. **$P < 0.01$
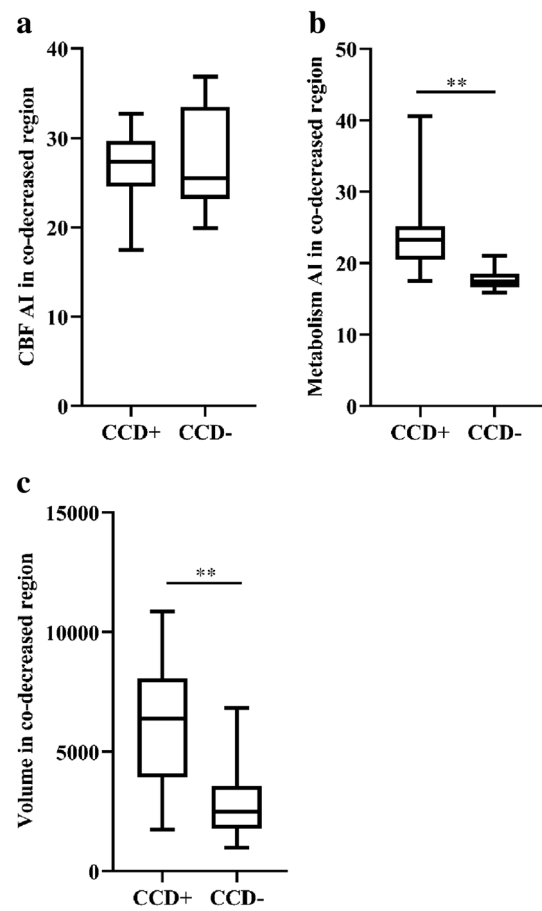

Fig. 5 Comparison of parameters in a co-decreased region between the two groups. No difference in the CBF AI **a** between the CCD-positive group and the CCD-negative group. There was significantly higher metabolism AI **b** and larger volume **c** in CCD-positive patients. **$P < 0.01$

patients (CCD + vs. CCD−: 23.03 vs. 17.43, $P = 0.003$; 6400.00 vs. 2491.00, $P = 0.005$). No significant difference in the CBF AI value was found in the co-decreased region between the two groups ($P = 0.733$) (Fig. 5). Detailed parameters of the CCD + and CCD− patients are shown in Table 2.

## Correlations between NIHSS and metabolism characteristics

The correlation analysis for these groups is shown in Fig. 6. Correlation analysis revealed that the preprocedural NIHSS score strongly correlated with the metabolism AI value in the decreased metabolism region ($r = 0.621$, $P = 0.001$) and the metabolism AI co-decreased region ($r = 0.571$, $P = 0.004$). A more modest but significant correlation was found between the volume of the decreased metabolism region ($r = 0.617$, $P = 0.001$) and the volume of the co-decreased region ($r = 0.497$, $P = 0.014$). No correlation was found between the

Table 2 Parameters in different regions between CCD+ and CCD− patients

	CCD+	CCD−	P value
Decreased blood flow region			
CBF AI (%), median (IQR)	25.84(4.93)	22.37(7.50)	0.591
Volume, median (IQR)	9839.50(4794.00)	8729.00(4943.75)	0.364
Decreased metabolism region			
Metabolism AI (%), median (IQR)	21.67(4.37)	16.78(0.99)	0.001
Volume, median (IQR)	9594.50(3947.75)	4353.00(2732.00)	<0.001
Co-decreased region			
CBF AI (%), median (IQR)	27.28(5.08)	25.50(10.28)	0.733
Metabolism AI (%), median (IQR)	23.03(4.70)	17.43(1.89)	0.003
Volume, median (IQR)	6400.00(4150.25)	2491.00(1814.00)	0.005

CCD crossed cerebellar diaschisis; *CBF* cerebral blood flow; *AI* asymmetry index; *IQR* interquartile range

Fig. 6 Correlations between neurological status and parameters. A significant correlation was observed between the NIHSS score and metabolism AI values in the decreased metabolism region ($r = 0.621$, $P = 0.001$) **a** and metabolism AI co-decreased region ($r = 0.571$, $P = 0.004$) **b** A more modest but significant correlation was found between the volume of the decreased metabolism region ($r = 0.617$, $P = 0.001$) **c** and the volume of the co-decreased region ($r = 0.497$, $P = 0.014$) **d**
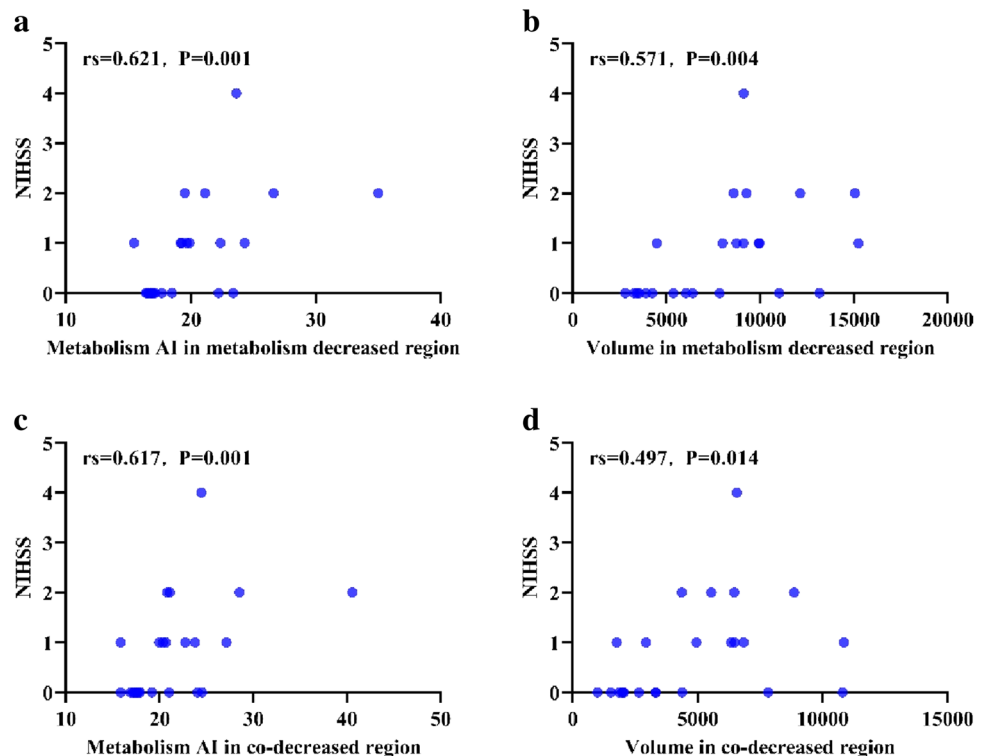
CBF AI and clinical outcome measures preoperatively or at the last follow-up.

Discussion

Cerebral perfusion and glucose metabolism are closely coupled to neural activity and are important markers of brain function. We retrospectively analyzed the ^{18}F-FDG PET/MR results of 24 patients with the chronic ischemic cerebrovascular disease before bypass surgery and added CCD as a factor for investigating the CCD-related supratentorial hemodynamic and metabolic status

before STA-MCA bypass surgery. Our results show that CCD may be an important factor in surgical selection in chronic symptomatic ischemic cerebrovascular disease.

Most previous reports mentioned CCD in patients with ischemic stroke [25, 26]. We found that 58% of the patients were CCD+, which is similar to the incidence reported by others [26, 27]. CCD is a common phenomenon when there is a supra-tentorial infarction. Although the size of the supra-tentorial infarctions in the CCD+ group was larger in our study, Sommer et al.[28] reported that the occurrence of CCD is influenced by the degree of the reduction of supratentorial perfusions rather than the size of the infarction.

For the quantitative assessment of the level of functional impairment following a stroke, NIHSS and mRS scores are used in neurological practice. Our results show that the CCD + patients had higher preprocedural NIHSS and mRS scores. Szilagyi et al. [29] reported that patients with CCD had worse clinical stroke scale values than patients without CCD in subacute stroke. Kunz et al. [30] also reported that subacute neurological function and recovery were worse in patients with CCD than in patients without CCD. Therefore, the early identification of patients with CCD may support appropriate management strategies and avoid potentially harmful treatments.

Bypass surgery aims to protect brain tissue from infarction by increasing blood flow and reducing the stroke risk in patients [31]. Bai et al. [4] demonstrated that STA-MCA bypass is an effective and safe way to improve the regional ischemic status in ischemic cerebrovascular diseases. However, Powers et al. [9] reported that bypass surgery combined with medical therapy did not reduce the risk of recurrent stroke compared to medical therapy alone. One of the indications of this surgery is cerebral supratentorial ischemic status. The occurrence of CCD is related to supratentorial blood flow or metabolism. However, few studies describing the relationship between CCD-related supratentorial blood flow and the metabolic status and bypass surgery outcomes are available. We added CCD as a factor to compare the CCD-related supratentorial hemodynamic and metabolic status. Our results suggest that no significant differences were observed in the follow-up NIHSS and mRS scores between the two groups at 1 year. NIHSS and mRS scores decreased significantly after surgery in the CCD + group. These results demonstrated that surgical treatment was beneficial to the recovery of patients with CCD.

Theoretically, insufficient blood flow and metabolic impairment resulting from vascular occlusion after an ischemic stroke can cause tissue damage [32]. The supratentorial ischemic status is an important indicator of surgery. In our study, we focused on evaluating non-infarcted regions based on structural images because in the chronic ischemic stage, structural imaging is negative except for infarction areas. The risk increases to 25% for patients with severe hemodynamic impairment. Most studies documented that a region with decreased blood flow was important for patients with ischemic cerebrovascular disease after surgery [4, 33, 34]. However, few studies have focused on the CCD-related degree and size of supratentorial decreased blood flow regions and surgical outcomes. Although the supratentorial parameters of the decreased blood flow region in the CCD + group were higher than those in the CCD− group before surgery, no significant differences were observed in the supratentorial volume of the decreased blood flow region and CBF AI

value between the two groups. Previous studies showed that ASL-MRI detected CCD with a relatively short PLD time (PLD = 1.5 s) [35, 36]. Long PLDs are required for ASL studies of supratentorial blood flow in the chronic stage [23]. The long PLD time selected by ASL and the supply of cerebral collateral circulation may have affected the results in this study [37]. We also found no correlation between the parameters in the decreased blood flow region and clinical outcome. Kunz et al. [30] demonstrated that the clinical score at the chronic stage was not available for all ischemic patients.

Maintaining normal brain homeostasis is a continuous energy-consuming process. In our previous study, 15 patients demonstrated improved glucose metabolism on ^{18}F-FDG PET/MR after bypass surgery [10]. Yu et al. [8] performed a serial PET study in which ^{18}F-FDG was used to investigate changes in glucose metabolism before and after bypass surgery and found that the uptake of ^{18}F-FDG in the hypoperfusion region surrounding the ischemic core was a sensitive indicator for predicting ischemia. The present study retrospectively analyzed glucose metabolic alterations between CCD + and CCD− groups before bypass surgery. Significant differences were detected in the preprocedural parameters of the metabolism-decreased region. Correlation analysis showed that the preprocedural NIHSS score strongly correlated with metabolic parameters in regions with decreased metabolism. A serial PET study with longitudinal follow-up at multiple time points after surgical therapy highlighted the usefulness of CCD as an indicator of clinical outcomes [38]. Our data indicated that the phenomenon of CCD may play a pivotal role in treatment selection in steno-occlusive artery disease.

Decreased blood flow and energy failure are the main pathophysiologies of cerebral ischemia [39, 40]. Previous studies have investigated the relationship between perfusion and glucose metabolism using separate PET and MR procedures [41, 42]. The advantage of our approach is that we avoided functional and physiological variations using different modalities. Using hybrid PET/MR, we focused on the CCD-related supratentorial blood flow and metabolic status before bypass surgery. We previously found that the areas with reduced blood flow and the areas with reduced metabolism are not completely overlapping. We defined the co-decreased region in terms of both decreased CBF values and lower ^{18}F-FDG uptake levels. The present study found there was a larger volume and a higher metabolism AI value in the CCD + group. The preprocedural clinical score had strong correlations with the metabolism AI value and volume of the co-decreased region. Although there was no statistical significance, the CBF AI value was slightly higher in the CCD + group. Paschen et al.[43] found that the

compensatory increase of glucose metabolism at rCBF between 20 and 35 ml/100 g/min was sharply reduced at rCBF <20 ml/100 g/min in an animal model of ischemia. Based on the mechanism of stroke, we propose that the co-decreased region may have a higher risk of infarction. Bypass surgery may reduce risks in patients with CCD-related supratentorial blood flow and metabolic status.

The present study also had some limitations. First, the study was retrospective, which did not allow a sample size estimation, but we expect that our results will be confirmed in larger prospective study cohorts. Second, multiple PLDs should have been chosen. Absolute quantitative parameters were not measured using dynamic ^{18}F-FDG PET on an integrated PET/MR system. Another limitation of this study was the lack of cerebellar quantification. Additionally, long-term PET/MR follow-up can help to monitor longitudinal hemodynamic and metabolic changes, which should be included in future prospective studies.

Conclusions

In summary, the results of our study suggest that cerebral hemodynamic and metabolic patterns are important indicators of CCD. CCD + patients with chronic ischemic cerebrovascular disease received a significant benefit from bypass surgery. Staging based on the CCD-related supratentorial blood flow and metabolic status by hybrid PET/MR may help to personalize treatment.

References

1. Wu S, Wu B, Liu M, Chen Z, Wang W, Anderson CS, et al. Stroke in China: advances and challenges in epidemiology, prevention, and management. Lancet Neurol. 2019;18:394–405.

2. Reynolds MR, Derdeyn CP, Grubb RL Jr, Powers WJ, Zipfel GJ. Extracranial-intracranial bypass for ischemic cerebrovascular disease: what have we learned from the carotid occlusion surgery study? Neurosurg Focus. 2014;36:E9.

3. Yamauchi H, Kagawa S, Kishibe Y, Takahashi M, Higashi T. Progressive cortical neuronal damage and extracranial-intracranial bypass surgery in patients with misery perfusion. AJNR Am J Neuroradiol. 2017;38:935–41.

4. Bai J, Zhao YL, Wang R, Zhang D, Wang S, Zhao JZ, et al. Regional cerebral perfusion and ischemic status after standard superficial temporal artery–middle cerebral artery (STA-MCA) bypass surgery in ischemic cerebrovascular disease. Childs Nerv Syst. 2012;28:579–86.

5. Low SW, Teo K, Lwin S, Yeo LL, Paliwal PR, Ahmad A, et al. Improvement in cerebral hemodynamic parameters and outcomes after superficial temporal artery-middle cerebral artery bypass in patients with severe stenoocclusive disease of the intracranial internal carotid or middle cerebral arteries. J Neurosurg. 2015;123:662–9.

6. Kao H, Lin M, Wu W, Tseng W, Su M, Chen Y, et al. Improvement of cerebral glucose metabolism in symptomatic patients with carotid artery stenosis after stenting. Clin Nucl Med. 2015;40:701–7.

7. Ma Y, Gu Y, Tong X, Wang J, Kuai D, Wang D, et al. The Carotid and Middle cerebral artery Occlusion Surgery Study (CMOSS): a study protocol for a randomised controlled trial. Trials. 2016;17:544.

8. Yu Z, Shi X, Zhou Z, Yang Y, Li P, Zhang Y. Cerebral glucose metabolism changes in chronic ischemia patients following subcranial-intracranial bypass. Neurosurg Rev. 2019;43:1383–9.

9. Powers WJ, Clarke WR, Grubb RL Jr, Videen TO, Adams HP Jr, Derdeyn CP. Extracranial-intracranial bypass surgery for stroke prevention in hemodynamic cerebral ischemia: the carotid occlusion surgery study randomized trial. JAMA. 2011;306:1983–92.

10. Cui B, Zhang T, Ma Y, Chen Z, Ma J, Ma L, et al. Simultaneous PET-MRI imaging of cerebral blood flow and glucose metabolism in the symptomatic unilateral internal carotid artery/middle cerebral artery steno-occlusive disease. Eur J Nucl Med Mol Imaging. 2020;47:1668–77.

11. Kim JS, Kim SH, Lim SH, Im S, Hong BY, Oh J, et al. Degeneration of the inferior cerebellar peduncle after middle cerebral artery stroke: another perspective on crossed cerebellar diaschisis. Stroke. 2019;50:2700–7.

12. Baron JC, Rougemont D, Soussaline F, Bustany P, Crouzel C, Bousser MG, et al. Local interrelationships of cerebral oxygen consumption and glucose utilization in normal subjects and in ischemic stroke patients: a positron tomography study. J Cereb Blood Flow Metab. 1984;4:140–9.

13. Wang J, Suo S, Zu J, Zhu W, Pan L, Song S, et al. Detection of crossed cerebellar diaschisis by intravoxel incoherent motion MR imaging in subacute ischemic stroke. Cell Transplant. 2019;28:1062–70.

14. Nocun A, Wojczal J, Szczepanska-Szerej H, Wilczynski M, Chrapko B. Quantitative evaluation of crossed cerebellar diaschisis, using voxel-based analysis of Tc-99m ECD brain SPECT. Nucl Med Rev Cent East Eur. 2013;16:31–4.

15. Uchino H, Kazumata K, Ito M, Nakayama N, Kuroda S, Houkin K. Crossed cerebellar diaschisis as an indicator of severe cerebral hyperperfusion after direct bypass for moyamoya disease. Neurosurg Rev. 2021;44:599–605.

16. Nahab F, Liu M, Rahman HA, Rangaraju S, Barrow D, Cawley CM, et al. Recurrent hemispheric stroke syndromes in symptomatic atherosclerotic internal carotid artery occlusions: the carotid occlusion surgery study randomized trial. Neurosurgery. 2020;87:137–41.

17. Gupta A, Chazen JL, Hartman M, Delgado D, Anumula N, Shao H, et al. Cerebrovascular reserve and stroke risk in patients with carotid stenosis or occlusion. Stroke. 2012;43:2884–91.

18. Hui L, Hui L, Tong H. Prediction of the long-term efficacy of STA-MCA bypass by DSC-PI. Transl Neurosci. 2016;7:110–5.

19. Grant AM, Deller TW, Khalighi MM, Maramraju SH, Delso G, Levin CS. NEMA NU 2–2012 performance studies for the SiPM-based ToF-PET component of the GE SIGNA PET/MR system. Med Phys. 2016;43:2334.

20. Zanaty M, Howard S, Roa JA, Alvarez CM, Kung DK, McCarthy DJ, et al. Cognitive and cerebral hemodynamic effects of endovascular recanalization of chronically occluded cervical internal carotid artery: single-center study and review of the literature. J Neurosurg. 2019;132:1–9.

21. Li H, Chen C, Li Z, Ling C, Sun J, Wang H. Superficial temporal artery-posterior cerebral artery bypass for the treatment of chronic basilar artery occlusion. World Neurosurg. 2021;150:e45-51.

22. Hou Y, Guo K, Fan X, Shang K, Wang J, Wang Z, et al. Crossed cerebellar diaschisis: risk factors and prognostic value in focal cortical dysplasia by (18)F-FDG PET/CT. Ann Nucl Med. 2021;35:719–27.

23. Fan AP, Guo J, Khalighi MM, Gulaka PK, Shen B, Park JH, et al. Long-delay arterial spin labeling provides more accurate cerebral blood flow measurements in Moyamoya patients: a simultaneous positron emission tomography/MRI study. Stroke. 2017;48:2441–9.

24. Miyazawa N, Toyama K, Arbab AS, Koizumi K, Arai T, Nukui H. Evaluation of crossed cerebellar diaschisis in 30 patients with major cerebral artery occlusion by means of quantitative I-123 IMP SPECT. Ann Nucl Med. 2001;15:513–9.

25. Kim SE, Choi CW, Yoon BW, Chung JK, Roh JH, Lee MC, et al. Crossed-cerebellar diaschisis in cerebral infarction: technetium-99m-HMPAO SPECT and MRI. J Nucl Med. 1997;38:14–9.

26. Komaba Y, Mishina M, Utsumi K, Katayama Y, Kobayashi S, Mori O. Crossed cerebellar diaschisis in patients with cortical infarction: logistic regression analysis to control for confounding effects. Stroke. 2004;35:472–6.

27. Sebok M, van Niftrik CHB, Piccirelli M, Bozinov O, Wegener S, Esposito G, et al. BOLD cerebrovascular reactivity as a novel marker for crossed cerebellar diaschisis. Neurology. 2018;91:e1328–37.

28. Sommer WH, Bollwein C, Thierfelder KM, Baumann A, Janssen H, Ertl-Wagner B, et al. Crossed cerebellar diaschisis in patients with acute middle cerebral artery infarction: occurrence and perfusion characteristics. J Cereb Blood Flow Metab. 2016;36:743–54.

29. Szilagyi G, Vas A, Kerenyi L, Nagy Z, Csiba L, Gulyas B. Correlation between crossed cerebellar diaschisis and clinical neurological scales. Acta Neurol Scand. 2012;125:373–81.

30. Kunz WG, Sommer WH, Hohne C, Fabritius MP, Schuler F, Dorn F, et al. Crossed cerebellar diaschisis in acute ischemic stroke: impact on morphologic and functional outcome. J Cereb Blood Flow Metab. 2017;37:3615–24.

31. Hecht N, Wessels L, Fekonja L, von Weitzel-Mudersbach P, Vajkoczy P. Bypass strategies for common carotid artery occlusion. Acta Neurochir (Wien). 2019;161:1993–2002.

32. Hu X, De Silva TM, Chen J, Faraci FM. Cerebral vascular disease and neurovascular injury in ischemic stroke. Circ Res. 2017;120:449–71.

33. Fierstra J, Maclean DB, Fisher JA, Han JS, Mandell DM, Conklin J, et al. Surgical revascularization reverses cerebral cortical thinning in patients with severe cerebrovascular steno-occlusive disease. Stroke. 2011;42:1631–7.

34. Jussen D, Zdunczyk A, Schmidt S, Rösler J, Buchert R, Julkunen P, et al. Motor plasticity after extra–intracranial bypass surgery in occlusive cerebrovascular disease. Neurology. 2016;87:27–35.

35. Chen S, Guan M, Lian HJ, Ma LJ, Shang JK, He S, et al. Crossed cerebellar diaschisis detected by arterial spin-labeled perfusion magnetic resonance imaging in subacute ischemic stroke. J Stroke Cerebrovasc Dis. 2014;23:2378–83.

36. Strother MK, Buckingham C, Faraco CC, Arteaga DF, Lu P, Xu Y, et al. Crossed cerebellar diaschisis after stroke identified noninvasively with cerebral blood flow-weighted arterial spin labeling MRI. Eur J Radiol. 2016;85:136–42.

37. Chen H, Wu B, Zhu G, Wintermark M, Wu X, Su Z, et al. Permeability imaging as a biomarker of leptomeningeal collateral flow in patients with intracranial arterial stenosis. Cell Biochem Biophys. 2014;71:1273–9.

38. Sobesky J, Thiel A, Ghaemi M, Hilker RH, Rudolf J, Jacobs AH, et al. Crossed cerebellar diaschisis in acute human stroke: a PET study of serial changes and response to supratentorial reperfusion. J Cereb Blood Flow Metab. 2005;25:1685–91.

39. Kaviarasi S, Yuba E, Harada A, Krishnan UM. Emerging paradigms in nanotechnology for imaging and treatment of cerebral ischemia. J Control Release. 2019;300:22–45.

40. Evans NR, Tarkin JM, Buscombe JR, Markus HS, Rudd JHF, Warburton EA. PET imaging of the neurovascular interface in cerebrovascular disease. Nat Rev Neurol. 2017;13:676–88.

41. Huisman MC, van Golen LW, Hoetjes NJ, Greuter HN, Schober P, Ijzerman RG, et al. Cerebral blood flow and glucose metabolism in healthy volunteers measured using a high-resolution PET scanner. EJNMMI Res. 2012;2:63.

42. Kawai N, Kawanishi M, Shindou A, Kudomi N, Yamamoto Y, Nishiyama Y, et al. Cerebral blood flow and metabolism measurement using positron emission tomography before and during internal carotid artery test occlusions: feasibility of rapid quantitative measurement of CBF and OEF/CMRO2. Interv Neuroradiol. 2012;18:264–74.

43. Paschen W, Mies G, Hossmann KA. Threshold relationship between cerebral blood flow, glucose utilization, and energy metabolites during development of stroke in gerbils. Exp Neurol. 1992;117:325–33.

Publisher's Note Springer Nature remains neutral with regard to jurisdictional claims in published maps and institutional affiliations.

Authors and Affiliations

Bixiao Cui[1,2] · Yi Shan[1,2] · Tianhao Zhang[3,4] · Yan Ma[5] · Bin Yang[5] · Hongwei Yang[1,2] · Liqun Jiao[5] · Baoci Shan[3,4,6] · Jie Lu[1,2]

[1]   Department of Radiology and Nuclear Medicine, Xuanwu Hospital, Capital Medical University, Beijing, China

[2]   Beijing Key Laboratory of Magnetic Resonance Imaging and Brain Informatics, Beijing, China

[3]   Institute of High Energy Physics, Beijing Engineering Research Center of Radiographic Techniques and Equipment, Chinese Academy of Sciences, Beijing, China

[4]   School of Nuclear Science and Technology, University of Chinese Academy of Sciences, Beijing, China

[5]   Department of Neurosurgery, Xuanwu Hospital, Capital Medical University, Beijing, China

[6]   CAS Center for Excellence in Brain Science and Intelligence Technology, Shanghai, China